

Quantum Chemical Studies on 3-Nitroanilinium Trichloroacetate

T. KAVITHA¹, G. PASUPATHI², M.K. MARCHEWKA³, G. ANBALAGAN⁴ and N. KANAGATHARA^{5,*}

¹Department of Physics, Arasu Engineering College, Kumbakonam-612 501, India

²PG and Research Department of Physics, AVVM Sri Pushpam College (Autonomous), Poondi, Thanjavur-613 503, India

³Institute of Low Temperature and Structure Research, Polish Academy of Sciences, 50-950, Wroclaw, 2, P.O Box 937, Poland

⁴Department of Nuclear Physics, University of Madras, Guindy Campus, Chennai-600 025, India

⁵Department of Physics, Saveetha School of Engineering, Saveetha University, Thandalam, Chennai-602 105, India

*Corresponding author: E-mail: kanagathara@gmail.com; kanagathara23275@gmail.com

Received: 14 August 2017;

Accepted: 29 September 2017;

Published online: 30 November 2017;

AJC-18671

The organic single crystals of 3-nitroanilinium trichloroacetate have been grown from water solvent by using slow evaporation technique. Single crystal X-ray diffraction studies confirmed that the grown crystal is built up of 3-nitroanilinium cations and trichloroacetate anions. It is also found that the crystal crystallizes in monoclinic crystal system with space group P2(1) and the lattice parameters are obtained as $a = 8.4618(5) \text{ \AA}$, $b = 6.4401(4) \text{ \AA}$, $c = 11.6623(8) \text{ \AA}$ and $Z = 2$. DFT-B3LYP/6-311++G(d,p) basis set is used to study the molecular structure of 3-nitroanilinium trichloroacetate. The existence of hydrogen bonding has been analyzed. The vibrational assignments and analysis of 3-nitroanilinium trichloroacetate have been performed and proved the existence of good correlation between the scaled theoretical and experimental wavenumbers. Natural bond orbital analysis have been carried out to study the stability of molecule. Frontier molecular orbital analysis has been done and discussed.

Keywords: 3-Nitroanilinium trichloroacetate, Hydrogen bond, HOMO-LUMO, Natural bond orbital.

INTRODUCTION

Organic non-linear optical (NLO) materials have versatile applications in many fields which includes telecommunications, optical signal processing and optical switching because of its large non-linear susceptibilities when compared with inorganic crystals. But these organic crystals have large optical absorption, less thermal and mechanical stability which makes them unsuitable for non-linear optical applications [1-6]. Intramolecular charge transfer and strong π -electron delocalization determines the non-linear properties of organic molecules. Nitroaniline is one such push-pull molecule shows the intramolecular charge transfer from its NH_2 and NO_2 group [7].

The *o*-, *m*- and *p*-disubstituted benzene derivative chromophores exhibit non-linear optical properties in both solid and solution state [8]. 3-Nitroaniline and its substituted benzene derivatives have been found to be an intensive area of research nowadays due to its low melting temperature and large microscopic second order non-linear susceptibilities. Similarly, trichloroacetic acid also exhibits the second harmonic generation and the literature survey revealed the versatility of this compound [9-11]. The experimental and theoretical research of nitroaniline and its derivatives were studied by many researchers [12-16]. In this report, 3-nitroanilinium trichloroacetate have been grown by

slow evaporation technique. Selvakumar *et al.* [17] studied the structural, optical and thermal properties of 3-nitroanilinium trichloroacetate. The linear and non-linear optical properties of 3-nitroanilinium trichloroacetate has been studied theoretically by Dadsetani *et al.* [7]. As far as the authors knowledge concerned, this is for the first time we report the computational studies on 3-nitroanilinium trichloroacetate with 6-311++G(d,p) basis set. Also, the electronic parameters like chemical hardness, softness and electronegativity have been obtained by using molecular frontier orbital energies. Natural bonding orbital analysis establishes the stability of molecule.

EXPERIMENTAL

Synthesis of 3-nitroanilinium trichloroacetate: 3-Nitroaniline (Aldrich, 99 %) and trichloroacetic acid (Aldrich, 95 %) were taken and prepared in the ratio of 1:1. The dissolved trichloroacetic acid was dissolved and added dropwise to the hot solution of 3-nitroaniline. The solution was then stirred well for nearly 7 h and allowed to cool at room temperature. Active charcoal was used to purify the solution and finally the solution was allowed to evaporate over the course for few days. The obtained colourless and transparent crystals of 3-nitroanilinium trichloroacetate is obtained (Fig. 1).



Fig. 1. Photograph of 3-nitroanilinium trichloroacetate crystal

Crystal structure analysis: Single crystal X-ray diffraction analysis of 3-nitroanilinium trichloroacetate has been carried out with graphite monochromatized Mo K_{α} ($\lambda = 0.71073 \text{ \AA}$) four circle KUMA KM-4 diffractometer equipped with a two-dimensional area CCD detector. A crystal of dimension ($0.31 \text{ mm} \times 0.28 \text{ mm} \times 0.21 \text{ mm}$) was used for the data collection and taken in sealed capillary tube. The ω -scan technique ($\Delta\omega = 0.75^\circ$) was used for the data collection for one image and the intensities were collected at room temperature $293(2)\text{K}$. KUMA-KM-4 CCD software performs the intensities integration and Lorentz and polarization effect [18]. SHELXTL program calculates the face-indexed analytical absorption [19] and 2093 reflections ($R_{\text{int}} = 0.0164$) were used for structure solution and refinement. The Fourier syntheses of SHELXTL-PLUS program was used to solve the structure of grown crystal [19], SHELXL 97 was used for the structure refinement [20]. Anisotropic and isotropic displacement parameters were included for all non-hydrogen and hydrogen atoms, respectively.

Vibrational spectral analysis: The vibrational spectral analysis of polycrystalline powders of 3-nitroanilinium trichloroacetate have been studied at room temperature. Bruker IFS-88 spectrometer is used to record FT-IR spectrum in the region $4000\text{-}80 \text{ cm}^{-1}$ with resolution kept at 2 cm^{-1} .

Computational studies: In the present study, DFT theoretical computations of 3-nitroanilinium trichloroacetate have been performed with the Gaussian 09 program by using 6-311++G(d,p) basis set [21].

The single crystal X-ray diffraction data is used for the present calculations. The structure of geometry is optimized with minimum energy and lack of imaginary wavenumbers gives better agreement with experimental values. The calculated relative molecular weight of atoms in particular mode was generated by command "freq=internal" as described in Gaussian manual. Theoretically, the infrared and Raman intensities were computed. All frequencies were scaled by 0.97 in DFT [22]. The theoretical spectra were obtained by the procedure proposed by Michalska and Wysokinski [23]. The second order interactions between the filled and vacant orbitals of different subsystem has been analyzed by NBO 3.1 program [24]. The graphic interpretations

of the mentioned properties were made by GaussView [25] program. HOMO and LUMO properties were obtained by B3LYP/6-311++ G(d,p) basis set and graphic illustrations of the isosurface with value equal to 0.001 was used.

RESULTS AND DISCUSSION

Optimized geometry: Single crystal X-ray diffraction study confirms that 3-nitroanilinium trichloroacetate crystal exhibit monoclinic with non-centrosymmetric space group $P2(1)$. The lattice parameters are calculated to be $a = 8.4618(5) \text{ \AA}$, $b = 6.4401(4) \text{ \AA}$, $c = 11.6623(8) \text{ \AA}$, $\alpha = 90^\circ$, $\beta = 103.732(6)^\circ$, $\gamma = 90^\circ$ and $V = 617.37(7) (\text{ \AA})^3$. The single crystal X-ray diffraction data and structure refinement parameters of 3-nitroanilinium trichloroacetate are listed in Table-1. Figs. 2 and 3 shows the molecular structure (ORTEP diagram) and the structure from single crystal XRD data of 3-nitroanilinium trichloroacetate, respectively. Fig. 4 shows the packing diagram of 3-nitroanilinium trichloroacetate. Based on the atom numbering scheme provided in the optimized structure (Fig. 5), structural parameters are calculated theoretically in gas phase and are listed in Table-2. Table-3 listed the various hydrogen bond geometrical parameters with their corresponding symmetry codes. In the studied compound, 3-nitroaniline molecule exists in the cationic form and trichloroacetic molecule in the mono-ionized state. The protonated amine group hydrogen atoms interacts with trichloroacetate anion *via* N-H...O interactions and its carboxylate group oxygen atoms acts as hydrogen bond acceptor. This results in forming an infinite chain occurs along crystallographic b direction. The hydrogen atom H(2N) of protonated 3-nitroaniline amino group

TABLE-1
CRYSTAL DATA AND STRUCTURE REFINEMENT FOR
3-NITROANILINIUM TRICHLOROACETATE CRYSTAL

Empirical formula	$\text{C}_6\text{H}_7\text{N}_2\text{O}_4\text{Cl}_3$
Formula weight (g mol^{-1})	301.51
Temperature (K)	293(2)
Wavelength (\AA)	0.71073
Crystal system	Monoclinic
Space group	$P2(1)$
a	$8.4618(5) \text{ \AA}$
b	$6.4401(4) \text{ \AA}$
c	$11.6623(8) \text{ \AA}$
α	$90.000(5)$
β	$103.732(6)$
γ	$90.000(5)$
V	$617.37(7) (\text{ \AA})^3$
Z	2
D_{calc} (Mg m^{-3})	1.622
Absorption coefficient (mm^{-1})	0.745
F(000)	304
Crystal size (mm)	$0.31 \times 0.28 \times 0.21$
Theta range for data collection ($^\circ$)	$4.02 - 26.36$
Index ranges	$h = -10 \rightarrow 10$; $k = -8 \rightarrow 5$; $l = -14 \rightarrow 14$
Reflections collected / unique	5725 / 2093
Completeness to θ	98.5%
Refinement method	Full-matrix least squares on F^2
Data/restraints/parameters	2093/15/184
Goodness of fit on F^2	1.160
Extinction coefficient	0.0091(18)
Largest differences peak and hole (e. \AA^{-3})	0.638 and -0.469

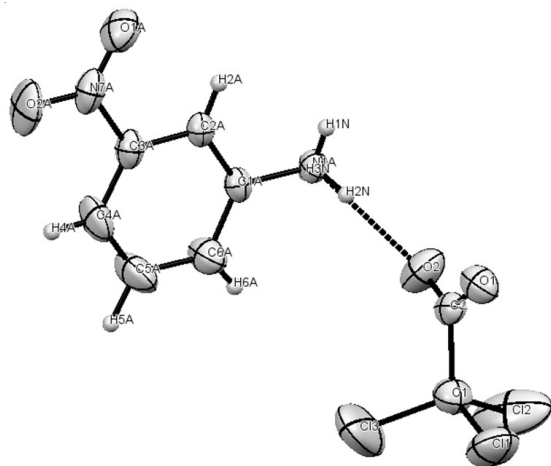


Fig. 2. ORTEP diagram of 3-nitroanilinium trichloroacetate

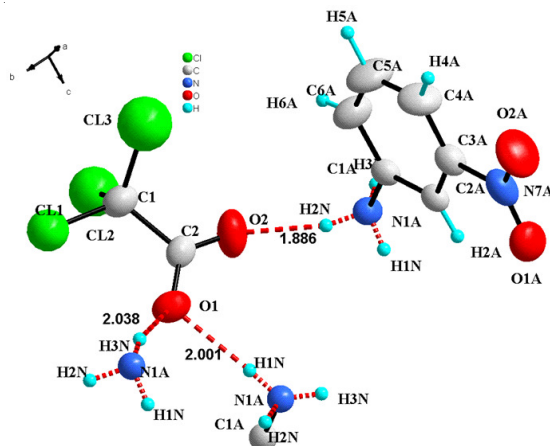


Fig. 3. Structure of 3-nitroanilinium trichloroacetate from single crystal XRD data

TABLE-2
GEOMETRICAL PARAMETERS OF 3-NITROANILINIUM TRICHLOROACETATE CRYSTAL

Bond length (Å)	B3LYP/6-311++G(d,p)	Expt. value	Bond angle (°)	B3LYP/6-311++G(d,p)	Expt. value	Bond angle (°)	B3LYP/6-311++g G(d,p)	Expt. value
R(1,7)	1.7651	1.763	A(5,3,6)	125.993	126.85	D(5,3,6,19)	-0.0323	-0.023
R(2,7)	1.7818	1.763	A(5,3,7)	122.6184	118.95	D(7,3,6,19)	179.924	169.64
R(3,5)	1.2006	1.220	A(6,3,7)	111.3885	115.09	D(5,3,7,2)	-120.765	-124.45
R(3,6)	1.3109	1.232	A(3,6,19)	108.6887	100.01	D(5,3,7,4)	119.734	114.55
R(3,7)	1.5517	1.550	A(1,7,2)	109.8339	106.24	D(6,3,7,1)	179.542	179.69
R(4,7)	1.782	1.741	A(1,7,3)	110.1402	111.80	D(6,3,7,2)	59.2772	59.05
R(6,19)	1.0028		A(1,7,4)	109.8686	107.80	D(6,3,7,4)	-60.2233	-62.95
R(8,9)	1.4173	1.456	A(2,7,3)	108.522	107.77	D(3,6,9,8)	-91.7176	-92.70
R(8,10)	1.3878	1.378	A(2,7,4)	110.0447	113.46	D(3,6,9,20)	22.537	21.05
R(8,15)	1.3944	1.369	A(3,7,4)	108.4037	109.78	D(3,6,9,21)	135.814	138.63
R(9,19)	1.7515		A(9,8,10)	120.3049	118.98	D(10,8,9,20)	151.168	150.63
R(9,20)	1.015	0.830	A(9,8,15)	119.9401	119.84	D(15,8,9,19)	72.1087	68.45
R(9,21)	1.0128	0.870	A(10,8,15)	119.6827	121.79	D(15,8,9,21)	-157.415	-163.01
R(10,12)	1.3834	1.389	A(8,9,19)	110.407	108.93	D(9,8,10,12)	177.253	179.39
R(10,18)	1.0818	0.884	A(8,9,20)	112.4711	106.89	D(9,8,10,18)	-2.6765	-1.75
R(11,13)	1.2158	1.224	A(8,9,21)	113.058	102.56	D(15,8,10,12)	0.3468	0.51
R(12,13)	1.4772	1.465	A(19,9,20)	94.408	92.11	D(15,8,10,18)	-179.583	-179.39
R(12,14)	1.382	1.389	A(19,9,21)	115.0382	116.90	D(9,8,15,17)	-177.27	-179.88
R(13,16)	1.2142	1.204	A(20,9,21)	110.1099	116.90	D(9,8,15,23)	2.1473	-1.63
R(14,17)	1.3873	1.366	A(8,10,12)	118.5694	119.37	D(10,8,5,23)	179.065	179.57
R(14,22)	1.08	0.927	A(8,10,18)	121.9468	120.95	D(8,10,12,13)	179.659	178.93
R(15,17)	1.3857	1.387	A(12,10,18)	119.4838	119.33	D(8,10,12,14)	-0.1499	-0.96
R(15,23)	1.084	0.860	A(10,12,13)	118.1133	117.26	D(18,10,12,14)	179.782	177.99
R(17,24)	1.0825	0.997	A(10,12,14)	122.97	122.98	D(10,12,13,11)	-0.4769	-1.60
			A(13,12,14)	118.9164	117.26	D(10,12,13,16)	179.584	178.02
			A(11,13,12)	117.6079	119.15	D(14,12,13,11)	179.341	178.31
			A(11,13,16)	124.7904	123.06	D(14,12,13,16)	-0.5984	-2.07
			A(12,13,16)	117.6016	117.78	D(10,12,14,22)	179.974	172.88
			A(12,14,17)	117.6732	118.42	D(13,12,14,17)	-179.857	-178.32
			A(12,14,22)	120.0562	120.05	D(12,14,17,15)	0.0491	0.73
			A(17,14,22)	122.2706	120.94	D(12,14,17,24)	-179.901	-177.00
			A(8,15,17)	120.2563	119.57	D(22,14,17,15)	-179.975	-171.95
			A(17,15,23)	120.4128	124.70	D(8,15,17,14)	0.1503	0.69
			A(14,17,15)	120.8475	120.31	D(8,15,17,24)	-179.899	-178.21
			A(14,17,24)	119.6572	115.46	D(23,15,17,14)	-179.26	-178.76

TABLE-3
SELECTED HYDROGEN GEOMETRICAL PARAMETERS

D-H...A	d(D-H)	d(H...A)	d(D...A)	∠(DHA)
N(1A)-H(2N)...O(2)	0.87(3)	1.89(3)	2.707(4)	156(3)
N(1A)-H(1N)...O(1) (i)	0.83(2)	2.00(2)	2.828(3)	174(3)
N(1A)-H(3N)...O(1) (ii)	0.81(3)	2.04(3)	2.804(4)	158(4)

Symmetry transformations used to generate equivalent atoms: (i) - x+2, y - 1/2, -z+2 (ii) x, y-1, z

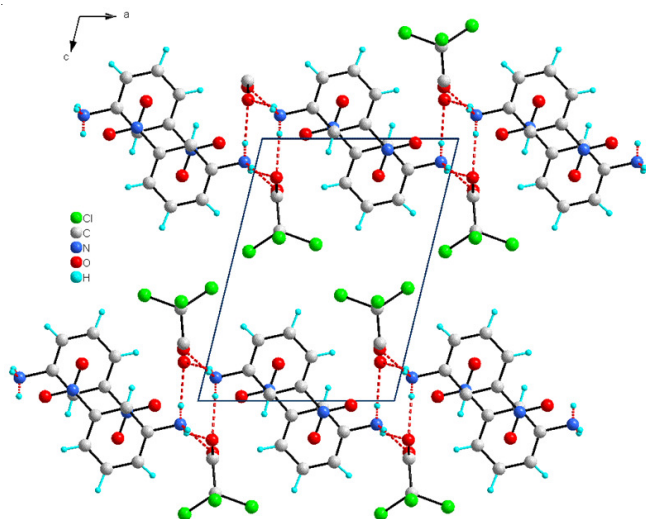


Fig. 4. Packing diagram of 3-nitroanilinium trichloroacetate

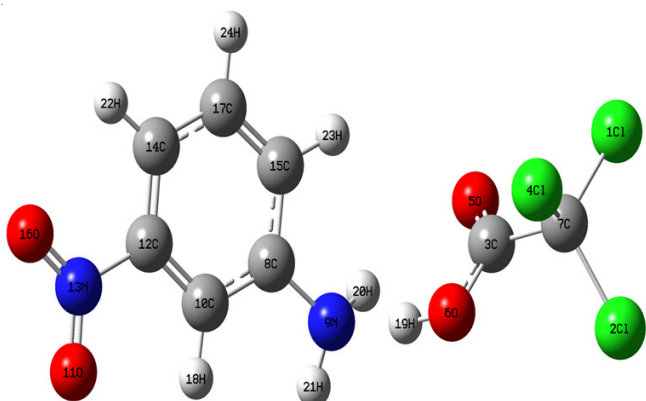


Fig. 5. Optimized structure of 3-nitroanilinium trichloroacetate

and trichloroacetate anion oxygen (O2) atom interacts through hydrogen bond N(1A)-H(2N)...O(2) with bond length 1.886 Å. The other hydrogen atoms H(1N) and H(3N) are involved in N(1A)-H(1N)...O(1) and N(1A)-H(3N)...O(1) hydrogen bond interaction, respectively with corresponding bond length of 2.001 Å and 2.038 Å. The ring C-C bond distances [C8-C10, C10-C12, C12-C14, C14-C17, C15-C8] are approximately in the range 1.38 Å whereas C3-C7 of trichloroacetate anion is small *i.e.* 1.5517 Å. It is observed that bond angle C10-C12-C14 where NO₂ group attached is 122.98°. But the bond angle between amino group and C10-C8-C15 is found to be 121.79°. Carbon atom (C8) attached to the protonated amino group forms an bond angle [C12-C10-C8, C17-C15-C8] of ~119° which is more than C12-C14-C17 (118°). This clearly shows that lone pair of electrons on the nitrogen of amino group in 3-nitroanilinium takes part in bond formation with the hydrogen of -COOH group of trichloroacetic acid. It is seen that almost the theoretical and experimental have similar results. However, the small deviations occurs due to the fact that theoretical calculations belong to isolated molecules has been done in gaseous phase and the experimental results were obtained in solid state.

Vibrational analysis: The vibrational frequencies of 3-nitroanilinium trichloroacetate have been computed by using optimized structural parameters with DFT-B3LYP/6-311++G(d,p) method. The measured FT-IR is shown in Fig. 6. Theoretically

computed vibrational spectrum of 3-nitroanilinium trichloroacetate is shown in Fig. 7. Table-4 listed the infrared wavenumbers and their relative intensities. The internal vibrations of 3-nitroanilinium cations and trichloroacetate anions are observed in the region 4000-200 cm⁻¹. Below 200 cm⁻¹ wavenumbers can be ascribed to lattice vibrations of the crystal.

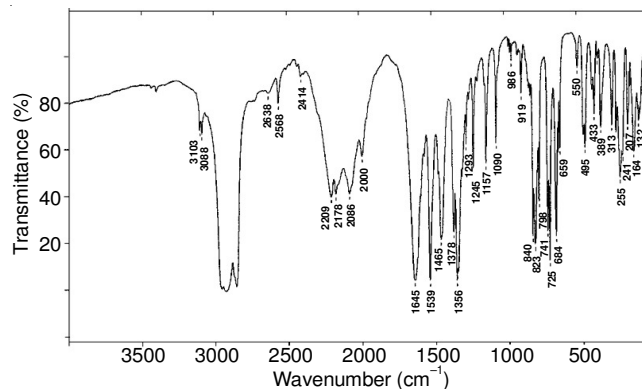


Fig. 6. FT-IR spectrum of 3-nitroanilinium trichloroacetate

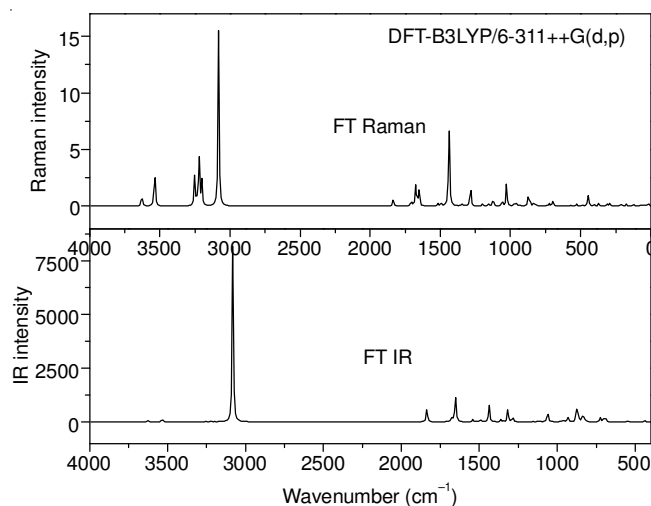


Fig. 7. Theoretical FT-IR and FT Raman spectrum of 3-nitroanilinium trichloroacetate

Vibrations of 3-nitroanilinium cations: The NH₂ group vibrations are described as the asymmetric stretching, symmetric stretching, scissoring, twisting, wagging and rocking vibrations are spread over a region. In 3-nitroanilinium trichloroacetate, the calculated scaled wavenumbers at 3517 and 3429 cm⁻¹ in B3LYP method are attributed to NH₂ antisymmetric stretching and symmetric stretching, respectively. A band at 3103 cm⁻¹ may be assigned to N-H asymmetric stretching frequency and this may overlap with aromatic C-H asymmetric stretching vibration [17]. The peaks noticed between 3100 and 3000 cm⁻¹ are due to aromatic CH stretching vibrations. The medium strong IR bands at 3088 and 3071 cm⁻¹ is attributed to CH asymmetric stretching vibration. DFT calculates these bands in between 3154-3103 cm⁻¹. The overtone and combination bands are noticed in the range 2638-2053 cm⁻¹. The NH₂ bending vibration in addition with C-C and N-O vibration are computed at 1657 and 1624 cm⁻¹ in DFT-B3LYP method. Experimentally obtained peaks at 1654 and 1623 cm⁻¹ with strong intensities. The NH₃⁺ asymmetric bending vibration is observed at 1567 cm⁻¹ with

TABLE-4
THEORETICAL AND EXPERIMENTAL VIBRATIONAL FREQUENCIES OF 3-NITROANILINIUM TRICHLOROACETATE

Experimental frequencies (cm ⁻¹)	B3LYP/6-311++G(d,p)		IR intensity	Raman intensity	Vibration band assignment
	Unscaled frequency	Scaled frequency			
	3626	3517	34.0366	39.4932	N-H ₂ asymmetric stretching
	3535	3429	43.5471	124.2199	N-H ₂ symmetric stretching
3103m	3251	3154	4.6989	79.3159	C-H asymmetric stretching
	3228	3131	4.9514	50.8514	C-H asymmetric stretching
3088m	3217	3120	1.9548	106.0759	C-H symmetric stretching
3071m	3199	3103	2.0791	58.6865	C-H symmetric stretching
2638s	3081	2989	2383.954	400.5944	O-H stretching
1774vw	1837	1782	245.9238	14.5911	COO - and OH stretching
1654vs	1708	1657	15.0974	8.6231	C-C, N-O, N-H stretching
1623s	1675	1624	80.0219	51.4211	C-C, N-O, N-H stretching
1567m	1659	1609	79.118	5.502	N-H ₂ bending
1527vs	1650	1600	319.2194	24.42	N-O2 stretching
	1541	1495	39.6027	0.4762	H-C-C bending
	1518	1472	4.2572	4.7989	H-C-C bending
	1492	1447	49.172	6.2833	C-O, O-H stretching
1357vs	1437	1393	281.8267	146.0446	NO ₂ stretching
1346vs	1361	1321	33.7882	1.186	C-C stretching
1300w	1343	1302	13.3745	3.3101	H-C-C bending
1218w	1315	1276	222.4126	1.0162	H-C-C bending
1171vw	1285	1246	88.8872	40.2232	H-C-C bending
1156vw	1199	1163	1.0461	3.3999	C-C stretching
1129vw	1158	1123	9.8342	3.5228	C-C stretching, H-N-H bending
1095w	1124	1091	24.4699	13.5715	C-N stretching
1074vw	1108	1075	9.0464	0.5842	C-C stretching
1002vw	1060	1029	193.6432	9.8535	O-C-O-H Torsion
986vw	1029	998	1.2719	25.3041	C-C-C bending
967vw	1026	995	1.9661	9.1118	C-C-C bending
945vw	978	948	8.107	2.3788	C-Cl ₃ stretching
924vw	963	934	27.1433	3.5383	C-C stretching
	958	929	4.0425	2.7389	C-C-C bending
917vw	933	905	84.9655	1.4939	C-C-C Torsion
890vw	875	848	98.4292	9.737	CCl ₃ stretching
841s	872	846	178.9324	7.1485	CCl ₃ stretching
825s	862	837	63.0756	7.4633	CCl ₃ stretching
813m	836	811	144.7192	5.7163	C-N-H bending
801m	819	795	35.6603	1.9606	C-N-H ; O-N-O bending
741s	739	716	7.4248	0.8433	O-C-O-N bending
730s	725	704	65.9327	4.3742	O-C-O-N bending
683s	702	681	75.1161	2.6892	Cl-C stretching
672m	697	676	9.8356	4.5953	C-C-C bending
663m	688	667	34.2424	0.2996	C-C-C- bending
555vw	571	554	1.1358	1.0015	O-N-C bending
512w	549	533	13.1653	0.7082	O-N-C bending
508w	527	511	2.4473	3.525	O-N-C bending
450vw	484	469	2.6016	2.1048	C-O-H bending
446vw	447	433	2.0386	13.726	O-N-C bending
437w	442	429	11.3436	2.0093	C-C-C-C Torsion
418vw	436	423	13.6849	1.5266	C-C-C-C Torsion
391w	402	390	0.9762	2.2102	C-C-C bending
383vw	371	360	4.9331	3.2767	Cl-C-Cl bending
313w	312	302	17.0059	3.2217	Cl-C-C-O Torsion
283w	293	285	2.5846	2.9514	Cl-C-Cl bending
279w	289	281	14.7385	1.2879	Cl-C-Cl bending
266w	262	254	1.9428	0.6501	Cl-C-Cl-C Torsion
243w	222	215	1.3278	0.7565	Cl-C-Cl-C Torsion
207w	211	205	20.4397	1.6234	L
200w	199	193	1.083	1.326	L
177w	174	169	0.4118	2.5828	L
	123	119	5.1414	2.5978	L
	72	70	3.6092	1.2056	L
	62	60	0.8599	0.6549	L
	53	51	2.697	0.3082	L
	41	40	0.1204	1.3394	L
	26	25	2.2048	2.4489	L
	13	13	0.4557	1.4616	L
	11	11	1.4707	1.2323	L

medium strong intensity. The band in the region around 1570-1500 and 1370-1300 cm^{-1} in nitrobenzene and substituted nitrobenzene are representing the asymmetric and symmetric stretching modes of NO_2 vibration, respectively [26,27]. The asymmetric stretching vibration of NO_2 group exhibits a band at 1527 cm^{-1} and the corresponding symmetric mode is observed at 1357 cm^{-1} with very strong intensities. Theoretically, their counterpart occurs at 1600 and 1393 cm^{-1} . The stretching vibrations of C-C and C-N exists in the range around 1600-1300 cm^{-1} . The infrared peak with weak intensity is ascribed to C-N stretching vibration. DFT calculates this C-N stretching vibration at 1091 cm^{-1} . The aromatic bending vibrations of C-H are observed around 1300-1100 cm^{-1} (in-plane) and 1100-900 cm^{-1} (out plane), respectively. In this report, C-H in plane and out plane bending modes are observed at 986 and 890 cm^{-1} , respectively with very weak intensities. The obtained vibrations are tabulated in Table-4. There exists a good conformity between theoretically computed vibrations and experimental observations.

Vibrations of trichloroacetate anions: The C-C mode of vibration in trichloroacetate anion is observed at 1346 and 1300 cm^{-1} with strong and weak intensities. Theoretically these peaks are computed at 1321 and 1302 cm^{-1} . The COO^- asymmetric vibration occurs at 1782 cm^{-1} and symmetric vibration occurs at 1447 cm^{-1} . Experimentally, this COO^- ion appears at 1774 cm^{-1} . The IR peak with strong intensity at 730 cm^{-1} is ascribed to C-Cl stretching vibration. Theoretically this peak is found at 681 cm^{-1} . The vibrational bands observed below 500 cm^{-1} are due to the skeletal vibrations. Theoretically, C-Cl3 stretching vibrations calculated at 848, 846 and 837 cm^{-1} . The ionized carboxylic group COO^- bending mode occurs at 741 cm^{-1} with strong intensity in the infrared spectrum. The trichloroacetate COO^- deformation peaks are observed at 681, 456, 446, 437 and 417 cm^{-1} [28].

Natural bonding orbital analysis: The inter- and intramolecular interactions between the bonds and the charge transfer between the molecules can be studied by natural bonding orbital (NBO) analysis. This can be done with the help of second order Fock matrix in NBO analysis [29-31]. The stabilization energy $E^{(2)}$ corresponding to the delocalization $i \rightarrow j$ is estimated as:

$$E^{(2)} = \Delta E_{ij} = q_i \frac{F(i,j)^2}{\epsilon_j - \epsilon_i}$$

where i represents donor and j represents acceptor.

The larger value of stabilization energy $E^{(2)}$ indicates the strong interaction between electron donors and electron acceptors of the system. This corresponds to the delocalization of electron density between lone pair of occupied and unoccupied NBO orbitals. Natural bonding orbital investigation has been carried out at DFT-B3LYP/6-311++G(d,p) level to explain the rehybridization, delocalization of the electron density and intra molecular interactions within the molecule. Fig. 8 shows the NBO charges of 3-nitroanilinium trichloroacetate. The H7, H8, and H9 atomic charges are smaller than H12 and H13 charges due to the presence of electronegative oxygen atom. The H16 and H17 atoms have more positive atomic charge than the other hydrogen atoms which is due to the presence of O17 and O19 electronegative oxygen atoms. The strong intramolecular interaction of between trichloroacetic acid molecule has stabilization

energy of 27.80 kJ/mol (LP(2)O5 \rightarrow BD*(1) C3-O6), 25.37 kJ/mol (LP(2)O5 \rightarrow BD*(1) C3-C7) and 57.92 kJ/mol (LP(2)O6 \rightarrow BD*(2) C3-O5). The other interactions are calculated and listed in Table-5. Similarly, within 3-nitroanilinium there exists a strong intramolecular interaction between O11 with π^* (N13-O16) leads to the maximum stabilization of 165.44 kJ/mol. Besides, π (C12-C14) NBO combined with π^* (C8-C10) and N13-O16 has stabilization energy of 20.10 and 22.95 kJ/mol, respectively. The other interactions between the bonding π (C15-C17) and (C8-C10) with antibonding π^* (C12-C14) has stabilization energy value as 20.47 and 22.04 kJ/mol, respectively. In 3-nitroanilinium trichloroacetate, the lone pair orbital N9 with π^* (O6-H19) orbital gives the strong stabilization to structure whose charge transfer energy value is 28.24 kJ/mol.

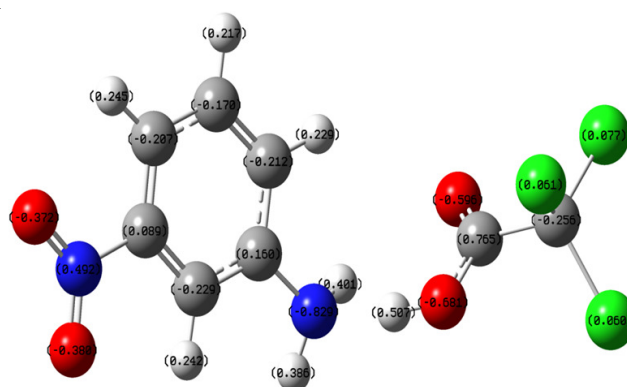


Fig. 8. NBO charges of 3-nitroanilinium trichloroacetate

TABLE-5
SECOND-ORDER PERTURBATION THEORY
ANALYSIS OF THE FOCK MATRIX IN NBO,
CALCULATED AT B3LYP/6-311++G(d,p)

Donor orbital (i)	Acceptor orbital (j)	$E^{(2)}$ (kcal/mol) ^a	$\epsilon_i - \epsilon_j$ (a.u.) ^b	F_{ij} (a.u.) ^c
LP(3) Cl 1	BD*(1) Cl 2-C7	6.77	0.40	0.047
LP(3) Cl 1	BD*(1) Cl 4-C7	6.83	0.40	0.047
LP(2) Cl 2	BD*(1) Cl 1- C7	6.45	0.42	0.047
LP(3)Cl 2	BD*(1) C4-C7	9.05	0.40	0.054
LP(2) Cl 4	BD*(1) Cl 1- C7	6.51	0.42	0.047
LP(3) Cl 4	BD*(1) Cl 2-C7	9.05	0.40	0.054
LP (2) O5	BD*(1) C3-O6	27.80	0.68	0.125
LP (2) O5	BD*(1) C3-C7	25.37	0.56	0.107
LP (1) O6	BD*(1)C3-O5	9.68	1.20	0.096
LP (2) O6	BD*(2) C3-O5	57.92	0.33	0.124
BD (2)C12-C14	BD*(2) C8-C10	20.10	0.29	0.068
BD (2)C12-C14	BD*(2) N13-O16	22.95	0.15	0.056
BD (2)C12-C14	BD*(2) C15-C17	18.85	0.30	0.067
BD (2)N13-O16	LP(3)O11	12.75	0.18	0.080
BD (1)C14-H22	BD*(1) C10-C12	4.64	1.09	0.064
BD (2)C15-C17	BD*(2) C8-C10	21.99	0.28	0.070
BD (2)C15-C17	BD*(2) C12-C14	20.47	0.28	0.069
BD (2)C8-C10	BD*(2) C12-C14	22.04	0.29	0.072
BD (2)C8-C10	BD*(2) C15-C17	18.45	0.30	0.067
BD (1)C12-C14	BD*(2) C10-C12	5.20	1.30	0.073
LP(1)N9	BD*(2)C8-C10	19.17	0.37	0.079
LP (2)O11	BD*(1) C12-N13	12.96	0.56	0.076
LP(2)O11	BD*(1) N13-O16	19.27	0.75	0.108
LP(3)O11	BD*(2)N13-O16	165.44	0.15	0.142
LP(2)O16	BD*(1) O11-N13	19.47	0.74	0.109
LP (2)O16	BD*(1) C12-N13	13.12	0.56	0.077
LP(1)N9	BD*(1) O6-H19	28.24	0.72	0.130

HOMO-LUMO analysis: The molecular electrical, optical properties and chemical reactions between the molecules is investigated by HOMO-LUMO analysis [32-35]. Fig. 9 shows the computed HOMO-LUMO of 3-nitroanilinium trichloroacetate by B3LYP/6-311++G(d,p) basis set. It is seen from Fig. 9 that HOMO electrons are delocalized on trichloroacetate anion. However, LUMO electrons are delocalized on the whole 3-nitroanilinium cation. The HOMO and LUMO energy gap equals to 7.04 eV indicates the occurrence of charge transfer in 3-nitroanilinium trichloroacetate [35]. The other electrical parameters like chemical potential (μ), electronegativity (χ), chemical hardness (η) and softness (S) are also calculated to measure the molecular stability and reactivity.

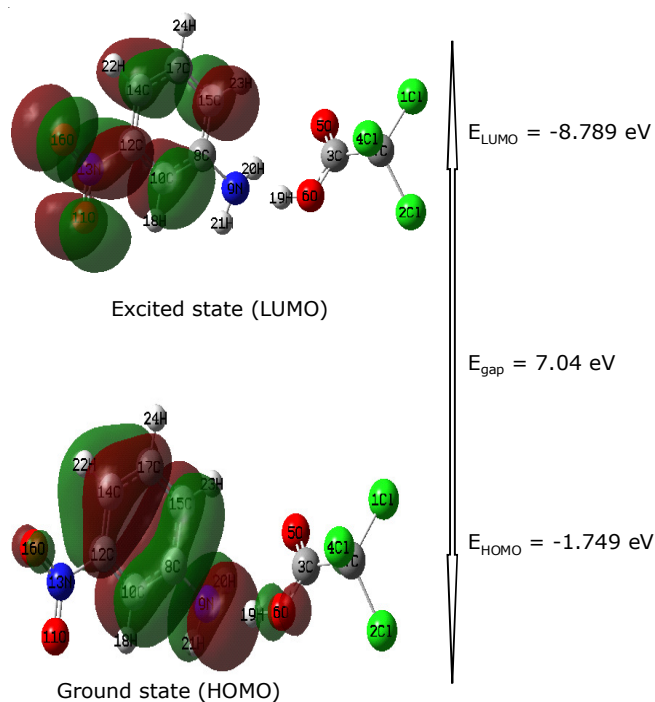


Fig. 9. HOMO-LUMO plot of 3-nitroanilinium trichloroacetate

The ionization energy and electron affinity can be expressed through HOMO and LUMO energies as $I = -E_{\text{HOMO}}$ and $A = -E_{\text{LUMO}}$. It is widely known that chemical hardness and softness are useful properties too. The small HOMO-LUMO gap of soft molecule is more reactive than hard molecule which has a bigger energy gap. The chemical hardness, softness, electro negativity and chemical potential results are found to be 3.52 eV, 0.1420 eV, 5.269 eV and -5.269 eV, respectively.

Density of states spectrum: In addition to HOMO-LUMO energy levels, quasi-degenerate energy levels can be seen in the neighbouring orbitals near the boundary region [36,37]. The total density spectrum of 3-nitroanilinium trichloroacetate (Fig. 10) was depicted using Gauss sum 2.2 program [38]. This spectrum gives the positive and negative charges to represent the visual representation of molecular orbital compositions and their chemical bonding contributions. In general, bonding interactions are given by positive value, antibonding interaction are given by negative value and zero represents the non-bonding interactions in DOS spectrum [39]. In the present study, bonding and anti-bonding interaction between the molecules are represented by positive and negative value, respectively.

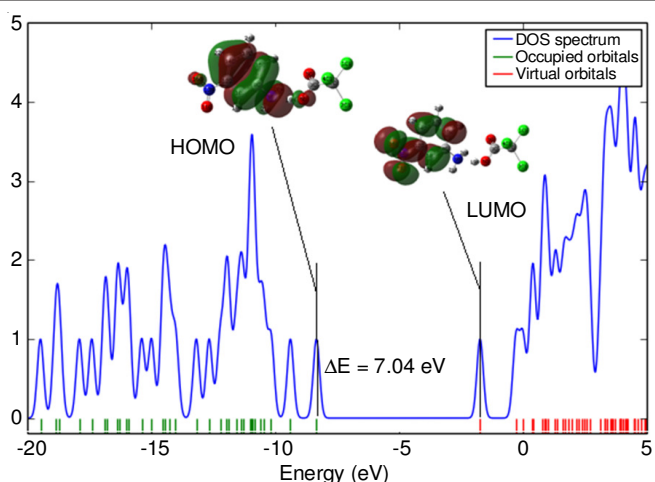


Fig. 10. DOS spectrum of 3-nitroanilinium trichloroacetate

Conclusion

3-Nitroanilinium trichloroacetate single crystals have been grown by the slow solvent evaporation method at room temperature. The obtained experimental X-ray diffraction data have been computed with the theoretical obtained values. The theoretical results revealed that the crystal structure well reproduces the optimized geometry and well matches with the experimental values. Theoretical calculations performed on the molecules provide clear-cut evidence for the vibrational spectrum and molecular parameters. The scaled values of vibrational wavenumbers have been compared with the experimental values, which in turn confirms that there exists an excellent matching between both the values. The molecular charge transfer interaction within the molecule is supported by HOMO-LUMO energy gap. The existence of N-H...O intermolecular interactions in the solid state has been confirmed by positive and negative potential sites in the molecular electrostatic potential surface. The reactive part in the molecule has been established by molecular electrostatic potential map.

Supplementary material

Full crystallographic data (cif file) relating to the crystal structure have been deposited with Cambridge Crystallographic Data centre as CCDC 1049311. Copies of this information can be obtained free of charge from Cambridge Crystallographic Data Centre, 12 Union Road, Cambridge CB2 1Ez, UK (Tel: +44(0) 1223 762911; E-mail: deposit@ccdc.cam.ac.uk; http://www.ccdc.cam.ac.uk)

REFERENCES

1. V.M. Geskin, C. Lambert and J.L. Bredas, *J. Am. Chem. Soc.*, **125**, 15651 (2003); <https://doi.org/10.1021/ja035862p>.
2. D. Sajan, H. Joe, V.S. Jayakumar and J. Zaleski, *J. Mol. Struct.*, **785**, 43 (2006); <https://doi.org/10.1016/j.molstruc.2005.09.041>.
3. A. Wojciechowski, K. Ozga, A.H. Reshak, R. Miedzinski, I.V. Kityk, J. Berdowski and Z. Tylczyński, *Mater. Lett.*, **64**, 1957 (2010); <https://doi.org/10.1016/j.matlet.2010.06.034>.
4. C.B. de Araújo, A.S.L. Gomes and G. Boudebs, *Reports Progr. Phys.*, **79**, 036401 (2016); <https://doi.org/10.1088/0034-4885/79/3/036401>.
5. D.S. Chemla and J. Zyss, *Non-Linear Optical Properties of Organic Molecules and Crystals*, Academic Press, Chap. 2 (1987).

6. G.D. Stucky, S.R. Marder and J.E. Sohn, *ACS Symp. Ser.*, **455**, Chap. 1, pp. 2-30 (1991); <https://doi.org/10.1021/bk-1991-0455.ch001>.
7. M. Dadsetani and A.R. Omid, *J. Phys. Chem. Solids*, **85**, 117 (2015); <https://doi.org/10.1016/j.jpccs.2015.05.011>.
8. A. Dulcic and C. Sauteret, *J. Chem. Phys.*, **69**, 3453 (1978); <https://doi.org/10.1063/1.437076>.
9. K. Rajagopal, R.V. Krishnakumar, A. Mostad and S. Natarajan, *Acta Crystallogr. Sect. E Struct. Rep. Online*, **59**, 277 (2003); <https://doi.org/10.1107/S1600536803002332>.
10. J. Baran, A.J. Barnes, B. Engelen, M. Panthofer, A. Pietraszko, H. Ratajczak and M. Sledz, *J. Mol. Struct.*, 550-551, 21-41 (2000); [https://doi.org/10.1016/S0022-2860\(00\)00381-1](https://doi.org/10.1016/S0022-2860(00)00381-1).
11. N. Kanagathara, N.G. Renganathan, M.K. Marchewka, N. Sivakumar, K. Gayathri, P. Krishnan, S. Gunasekaran and G. Anbalagan, *Spectrochim. Acta A*, **101**, 112 (2013); <https://doi.org/10.1016/j.saa.2012.09.057>.
12. V. Krishnakumar and V. Balachandran, *Spectrochim. Acta A*, **61**, 1811 (2005); <https://doi.org/10.1016/j.saa.2004.07.012>.
13. M. Honda, A. Fujii, E. Fujimaki, T. Ebata and N. Mikami, *J. Phys. Chem. A*, **107**, 3678 (2003); <https://doi.org/10.1021/jp022504k>.
14. R. Shankar, R.A. Yadav, I.S. Singh, O.N. Singh and J. Indian, *Pure Appl. Phys.*, **23**, 339 (1985).
15. E. Kavitha, N. Sundaraganesan and S. Sebastian *Indian J. Pure Appl. Phys.*, **48**, 20 (2010).
16. V. Arjunan, M.K. Marchewka, A. Pietraszko and M. Kalaivani, *Spectrochim. Acta A*, **97**, 625 (2012); <https://doi.org/10.1016/j.saa.2012.07.018>.
17. E. Selvakumar, A. Chandramohan, G. Anandha Babu and P. Ramasamy, *J. Cryst. Growth*, **401**, 323 (2014); <https://doi.org/10.1016/j.jcrysgro.2013.10.053>.
18. K. Diffraction, KM4/CCD Users' Guide, Version 1.169, Wroclaw, Poland (2000).
19. G.M. Sheldrick, SHELXL, Program for Crystal Structure Refinement, University of Göttingen, Germany (1993).
20. G.M. Sheldrick, *Acta Cryst. A*, **64**, 112 (2008); <https://doi.org/10.1107/S0108767307043930>.
21. M.J. Frisch, G.W. Trucks, H.B. Schlegel, G.E. Scuseria, M.A. Robb, J.R. Cheeseman, G. Scalmani, V. Barone, G. A. Petersson, H. Nakatsuji, X. Li, M. Caricato, A. Marenich, J. Bloino, B.G. Janesko, R. Gomperts, B. Mennucci, H.P. Hratchian, J.V. Ortiz, A.F. Izmaylov, J.L. Sonnenberg, D. Williams-Young, F. Ding, F. Lipparini, F. Egidi, J. Goings, B. Peng, A. Petrone, T. Henderson, D. Ranasinghe, V.G. Zakrzewski, J. Gao, N. Rega, G. Zheng, W. Liang, M. Hada, M. Ehara, K. Toyota, R. Fukuda, J. Hasegawa, M. Ishida, T. Nakajima, Y. Honda, O. Kitao, H. Nakai, T. Vreven, K. Throssell, J.A. Montgomery Jr., J.E. Peralta, F. Ogliaro, M. Bearpark, J.J. Heyd, E. Brothers, K.N. Kudin, V.N. Staroverov, T. Keith, R. Kobayashi, J. Normand, K. Raghavachari, A. Rendell, J.C. Burant, S.S. Iyengar, J. Tomasi, M. Cossi, J.M. Millam, M. Klene, C. Adamo, R. Cammi, J.W. Ochterski, R.L. Martin, K. Morokuma, O. Farkas, J.B. Foresman and D.J. Fox, Gaussian 09, Revision A.02, Gaussian, Inc., Wallingford CT (2009).
22. A.P. Scott and L. Radom, *J. Phys. Chem.*, **100**, 16502 (1996); <https://doi.org/10.1021/jp960976r>.
23. D. Michalska and R. Wysokiński, *Chem. Phys. Lett.*, **403**, 211 (2005); <https://doi.org/10.1016/j.cplett.2004.12.096>.
24. E.D. Glendenning, A.E. Reed, J.E. Carpenter and F. Einhold, NBO version 3.1, TCI, University of Wisconsin, Madison (1998).
25. R. Dennington, T. Keith and J. Millam, G. View, Version 5, Semichem Inc., Shawnee Mission KS (2009).
26. J.H.S. Green and D.J. Harrison, *Spectrochim. Acta A Mol. Biomol. Spectrosc.*, **26**, 1925 (1970); [https://doi.org/10.1016/0584-8539\(70\)80130-1](https://doi.org/10.1016/0584-8539(70)80130-1).
27. J.H. Green and H.A. Lauwers, *Spectrochim. Acta A*, **27**, 817 (1971); [https://doi.org/10.1016/0584-8539\(71\)80160-5](https://doi.org/10.1016/0584-8539(71)80160-5).
28. M.S. Soliman, *Spectrochim. Acta A*, **49**, 183 (1993); [https://doi.org/10.1016/0584-8539\(93\)80173-8](https://doi.org/10.1016/0584-8539(93)80173-8).
29. M. Szafran, A. Komasa and E. Bartoszak-Adamska, *J. Mol. Struct.*, **827**, 101 (2007); <https://doi.org/10.1016/j.molstruc.2006.05.012>.
30. C. James, A.A. Raj, R. Reghunathan, V.S. Jayakumar and I.H. Joe, *J. Raman Spectrosc.*, **37**, 1381 (2006); <https://doi.org/10.1002/jrs.1554>.
31. J. Liu, Z. Chen and S. Yuan, *J. Zhejiang Univ. Sci.*, **6B**, 584 (2005); <https://doi.org/10.1631/jzus.2005.B0584>.
32. J. Fleming, *Frontier Orbitals and Organic Chemical Reactions*, Wiley, London (1976).
33. T. Karakurt, M. Dincer, A. Çetin and M. Sekerci, *Spectrochim. Acta A*, **77**, 189 (2010); <https://doi.org/10.1016/j.saa.2010.05.006>.
34. K. Fukui, *Science*, **218**, 747 (1982); <https://doi.org/10.1126/science.218.4574.747>.
35. R.G. Pearson, *J. Am. Chem. Soc.*, **107**, 6801 (1985); <https://doi.org/10.1021/ja00310a009>.
36. R. Hoffmann, *Solids and Surfaces: A Chemist's View of Bonding in Extended Structures*, VCH Publishers, New York (1988).
37. J.G. Malecki, *Polyhedron*, **29**, 1973 (2010); <https://doi.org/10.1016/j.poly.2010.03.015>.
38. N.M. O'Boyle, A.L. Tenderholt and K.M. Langner, *J. Comput. Chem.*, **29**, 839 (2008); <https://doi.org/10.1002/jcc.20823>.
39. M. Chen, U.V. Waghmare, C.M. Friend and E. Kaxiras, *J. Chem. Phys.*, **109**, 6854 (1998); <https://doi.org/10.1063/1.477252>.